The Journal of Physical Chemistry A

 VOLUME 103, NUMBER 9, MARCH 4, 1999

LETTERS

Laser Photothermal Melting and Fragmentation of Gold Nanorods: Energy and Laser Pulse-Width Dependence

S. Link, C. Burda, M. B. Mohamed, B. Nikoobakht, and M. A. El-Sayed*

Laser Dynamics Laboratory, Georgia Institute of Technology, School of Chemistry and Biochemistry, Atlanta, Georgia 30332-0400

Received: July 23, 1998; In Final Form: January 12, 1999

We studied the shape transformation (by use of TEM and optical absorption spectroscopy) of gold nanorods in micellar solution by exposure to laser pulses of different pulse width (100 fs and 7 ns) and different energies (μJ to mJ) at 800 nm, where the longitudinal surface plasmon oscillation of the nanorods absorb. At moderate energies, the femtosecond irradiation melts the nanorods to near spherical particles of comparable volumes while the nanosecond pulses fragment them to smaller near-spherical particles. At high energies, fragmentation is also observed for the femtosecond irradiation. A mechanism involving the rate of energy deposition as compared to the rate of electron−phonon and phonon−phonon relaxation processes is proposed to determine the final fate of the laser-exposed nanorods, i.e., melting or fragmentation.

Introduction

Due to their potential technological applications, the synthesis and study of nanoparticles has been a very active field of research.[1−5] These studies of nanostructured materials show a strong dependence of their properties on size and shape. One of these properties is their melting behavior. A large volume of research was carried out on the size-dependence of the melting temperature of nanoparticles.[6−12] It is now clearly shown both experimentally[6−9] and theoretically[10−12] that (1) the near spherical nanoclusters melt at reduced temperatures compared to the bulk, (2) melting initially occurs at the surface, where the atoms are less bound, and (3) the melting-point depression is inversely proportional to the radius of the nanoparticle. Recently, the synthesis of cubic, tetrahedral, and other shapes of platinum nanoparticles in colloidal solution has been reported,[13] and the dependence of the surface melting temperature of these particles with different shapes has been studied.[14]

Other often-discussed features of nanoparticles are their optical properties. For example, spherical gold nanoparticles show a strong surface plasmon absorption[15−18] in the visible region at 520 nm resulting from the coherent oscillation of the free 6s electrons in the conduction band. This absorption is absent for very small particles (2 nm and smaller) as well as in bulk gold. For gold nanorods (NRs), the plasmon resonance splits into two modes:[15] one longitudinal mode along the long axis of the NR and a transverse mode perpendicular to the first. The maximum of the longitudinal surface plasmon absorption red shifts with increasing aspect ratio (length divided by the width) of the NRs. While the longitudinal mode is very sensitive to the aspect ratio, the maximum of the transverse surface plasmon oscillation is hardly effected by it. Gold NRs have been successfully synthesized by electrodeposition of gold into nanoporous alumina[19−21] and by an electrochemical method with the aid of shape-inducing micelles.[22]

Recently, the fragmentation of 40−60 nm silver nanodots after irradiation of their colloidal solutions with 355 nm picosecond laser pulses was reported.[23] The authors explained their observation with a model in which the ejection of electrons is one of the primary photochemical events leading to the

10.1021/jp983141k CCC: $18.00
Published on Web 03/04/1999

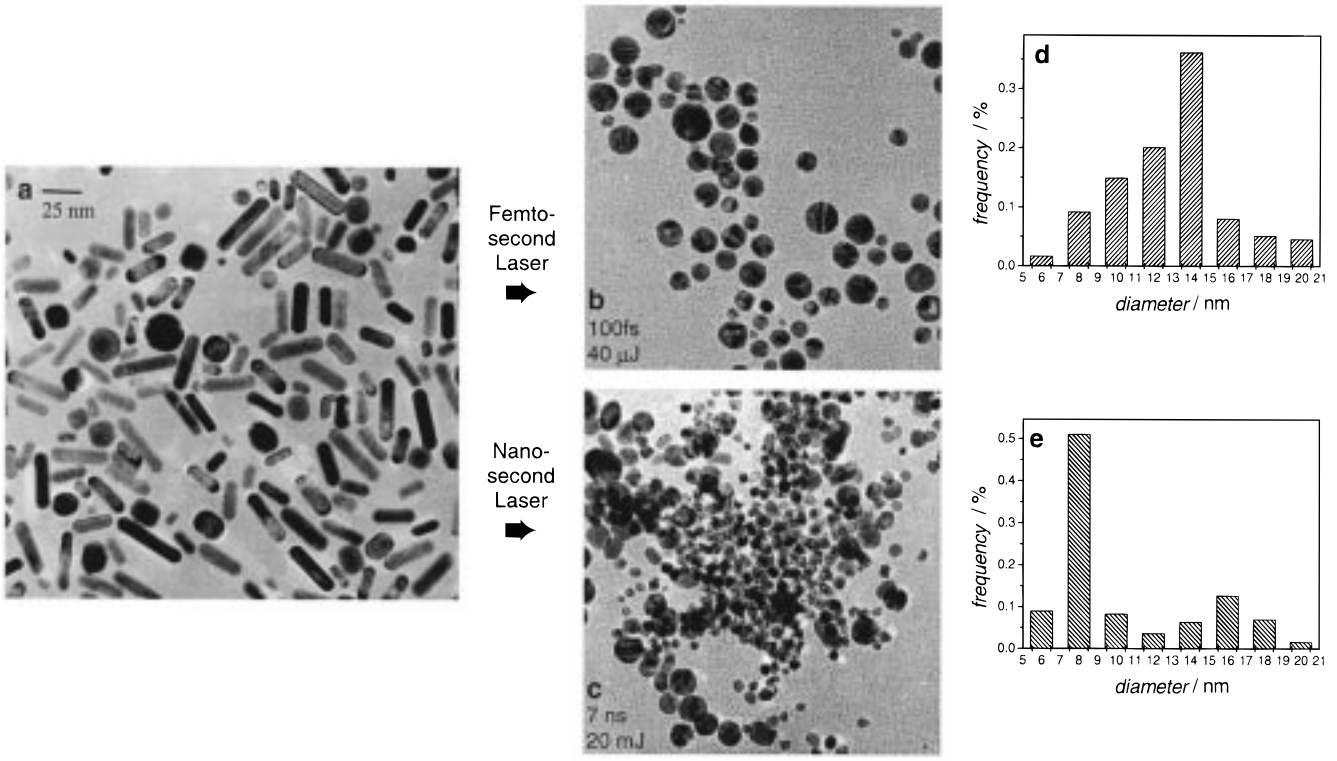

Figure 1. TEM images showing the effect of laser heating on the shape of gold nanorods encapsulated in micelles and dissolved in solution. (a) TEM image of the evaporated original solution prior to irradiation. (b) TEM image of the corresponding solution after exposure to 40 μJ femtosecond pulses (800 nm, 100 fs) for 7 min. The nanorods are transformed into near-spherical nanocrystals. (c) TEM image of the evaporated solution after exposure to 20 mJ nanosecond laser pulses (800 nm, 7 ns) for 1 min. Here, the irradiation fragments the nanorods into small near spherical nanocrystals. It is shown that the difference in action of the two types of laser pulses is due to the fact that the hot electrons resulting from the laser excitation heat the lattice in the dark in the femtosecond experiment (3 ps) but during the pulse in the nanosecond exposure. Further photon absorption by the hot lattice in the latter leads to an increase in the internal energy and fragmentation. (The scale bar in the upper left corner of (a) corresponds to 25 nm and also applies for b and c.)

photofragmentation process. In another study, spherical gold nanoparticles in solution were excited with 532 nanosecond pulses, which also led to fragmentation.[24] Thermal effects are thought to be responsible in this study as the laser heating leads to extremely high temperatures of the gold nanoparticles in a short time.

We report here for the first time on the photothermal stability of colloidal gold NRs to laser irradiation. Two types of lasers operating at a wavelength of 800 nm (corresponding to the maximum of the longitudinal plasmon band of the NRs) were used for heating the NRs: one was a 100 fs laser generating high peak power pulses and the other was a 7 ns high-energy laser. The shape changes occurring as a result of laser heating were monitored as a function of exposure time and laser energy by two techniques. In one, we measured the changes in the optical wavelength, the intensity, and band width of the two plasmon absorption bands of the colloidal NR solutions (transverse mode at 520 nm and longitudinal mode around 800 nm), which are sensitive to the shape of the NRs after laser exposure. In the second method, the shape and size distributions of the nanoparticles of the exposed colloidal solutions are determined from transmission electron microscopy (TEM) images of the deposited and dried nanoparticle samples. We found that the observed structural changes in the NRs are both laser pulse-width and energy (and thus power) dependent. The possible mechanisms responsible for the photothermal shape changes of the NRs are discussed in terms of the rate of energy deposition and electron−phonon and phonon−phonon relaxation times in the gold NRs as compared to the pulse width of the laser used.

Experimental Section

The gold NRs were prepared in micelles using an electrochemical method described previously by Wang et al.[16] The electrochemical cell is made of a gold (anode) and platinum (cathode) plate. The electrolyte solution consisted of a hydrophilic cationic surfactant, hexadecyltrimethylammonium bromide, and a hydrophobic cationic cosurfactant, tetradecylammonium bromide or tetraoctylammonium bromide. The electrolysis was carried out for 45 min with an applied current of 5 mA at a temperature of 42 °C under constant ultrasonication. The NRs were separated from spherical nanoparticles by centrifugation. Two NR samples were prepared by this procedure for the studies presented here. One sample consisted of gold NRs with an average length of 31 nm and a width of 8 nm. The mean aspect ratio was 3.75, and the maximum of the longitudinal plasmon absorption was located at 740 nm. The second preparation yielded NRs, 44 nm long and 11 nm wide, with a mean aspect ratio of 4.1 nm and an absorption maximum at 800 nm.

A 400 μL sample of the gold solution prepared in this way was then placed in a cylindrical cell with a path length of 2 mm. The sample cell was rotated in order to constantly mix the colloidal NR solution. The femtosecond pulses were generated by an amplified Ti:Sapphire laser system (Clark MXR, CPA 1000) which was pumped by an argon ion laser (Coherent, Innova 300). Laser pulses of 100 fs duration (hwfm) and an energy of 1 mJ at 800 nm with a repetition rate of 1 kHz were produced. The pulse energy was attenuated by apertures and neutral density filters, and the beam was then focused to a spot size of about 25 μm. The exposure time was controlled by a

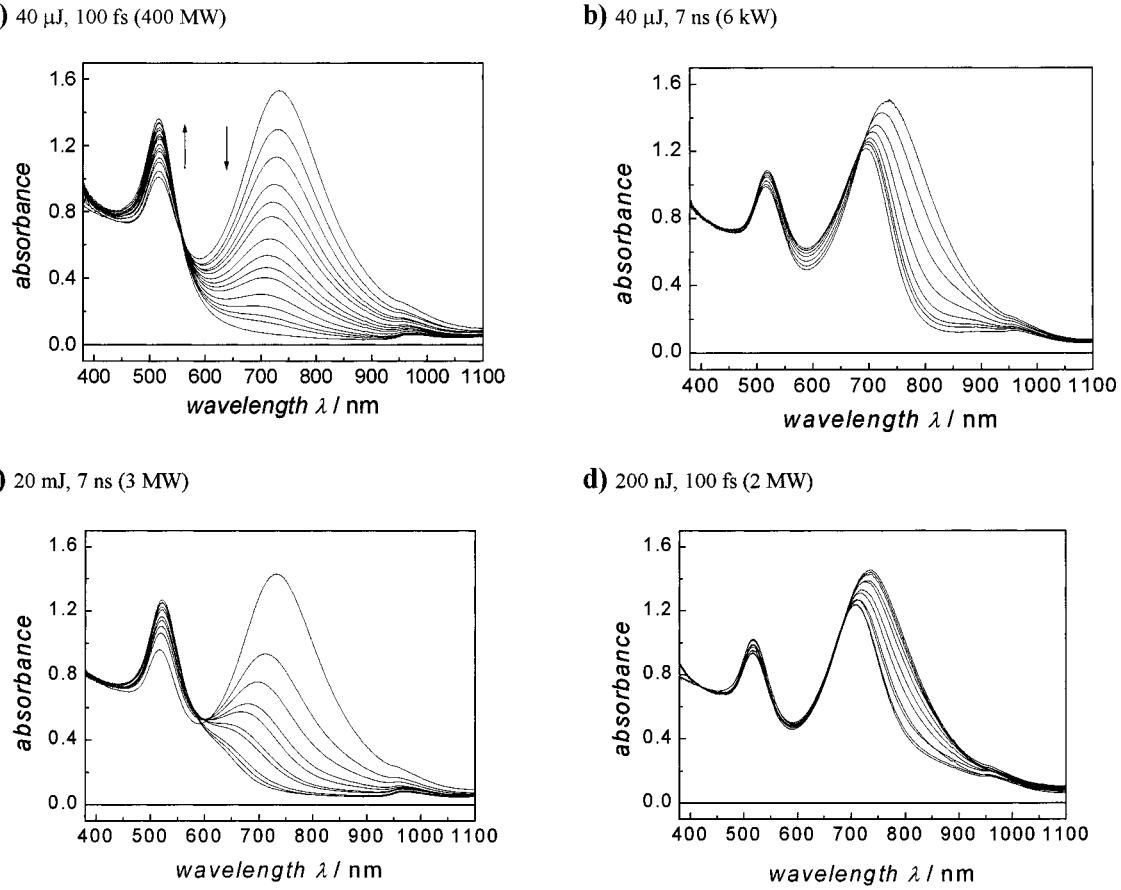

Figure 2. Monitoring the laser-induced shape changes of gold nanorods by observing the changes in their surface plasmon absorption spectra as a function of exposure time. Exposure to 40 μJ femtosecond laser pulses (a) reduces the intensity of the longitudinal band and increases the intensity of the 520 nm band due to the absorption of the spheres. Thus, it changes the rods into spheres. In (c), the results of the exposure to the high-energy (20 mJ) nanosecond laser pulses is shown. The longitudinal absorption band changes its maximum to shorter wavelength but retains its width, suggesting that the laser exposure changes the distribution into smaller rods and with increasing exposure time finally into spheres, as shown from the TEM image in Figure 1c. Both the low-energy nanosecond (b) and femtosecond (d) laser pulses lead to removing the long rods, as observed from the narrowing of the band width of the longitudinal band at 740 nm on its long-wavelength edge. (This effect can be used to obtain a narrow distribution of nanorods by photothermal laser shaping.) Note that the same per pulse energy leads to different results when the nanorods are exposed to femtosecond (a) and nanosecond (b) laser pulses.

shutter. The UV−vis absorption spectra were recorded after different exposure times on a Beckman DU 650 spectrophotometer.

An identical optical setup was used for the irradiation experiments with the nanosecond pulses. The laser source in this case was an optical parametric oscillator (Spectra Physics, MOPO-730) which was pumped by the third harmonic (355 nm) of a Nd:YAG laser (Spectra Physics, GCR-250). The output pulses had a pulse duration of about 7 ns and a repetition rate of 10 Hz and were tunable from 225 nm to 1.8 μm. The pulse energy was typically in the mJ range. To match the photon energy used in the femtosecond experiment, the idler wave at 800 nm was used as a light source in our experiments. Care was also taken to focus the nanosecond beam to the same spot size as in the femtosecond experiment.

The size and shape distributions of the particles formed in solution at different times of irradiation were determined from the TEM images of the evaporated solutions on carbon-coated copper grids. A Hitachi HF-2000 field emission TEM operating at 200 kV was used. Normally, 300−600 particles were counted in determining the distributions in each sample.

Results

Figure 1a shows the TEM image of the NR sample with a mean aspect ratio of 3.75 prior to the laser irradiation. Figure 1b illustrates the effect of the exposure to femtosecond laser pulses with an energy of 40 μJ. It is obvious that all the NRs have been converted into spheres. Analysis of the volume changes shows that, on average, the spheres formed have comparable volumes to those of the NRs with a mean particle diameter of 13 nm, as shown from the size histogram in Figure 1d. The effect of irradiating the NRs with the nanosecond laser having an energy of 20 mJ per pulse is given in Figure 1c. The TEM image shows that spheres are also formed but they have a much smaller volume than those of the initial NRs, suggesting that fragmentation has occurred. This is clear from the size histogram in Figure 1e, which shows that the mean particle diameter produced by irradiation with the nanosecond laser is 10 nm.

From Figure 1 it is not clear whether it is the difference in the laser energy, in the pulse width, or in the power that causes the observed difference in the products produced by exposure to the femtosecond and nanosecond lasers. To determine the important parameters, a series of experiments are carried out in which the same sample is exposed to femtosecond and nanosecond laser pulses of different energies. Optical spectroscopy is used in this study to follow the effect of the laser irradiation on the gold NR solutions. There already exists[25] a correlation between the maximum of the longitudinal absorption and the average rod length or aspect ratio. It is also established[25]

that when spheres are formed, the absorption at 520 nm (where the transverse plasmon absorption of the NRs absorbs) increases irrespective of the original NR length. The results of the effect of laser pulse width and energy on the optical absorption spectrum of the micellar aqueous solutions of the gold NRs are summarized in Figure 2.

Figure 2a and 2b compare the results of two experiments carried out with the same energy but two different pulse widths. In both experiments the laser pulses have the same energy of 40 μJ but due to the difference in their pulse widths (and thus power) the femtosecond laser seems to destroy all the NRs in the whole NR distribution into spheres. This is concluded from the observed decrease in the broad band due to the longitudinal absorption of the NRs at 800 nm and the increase in the band at 520 nm due to the absorption of the spheres in Figure 2a with increasing exposure time. This is also confirmed with the TEM images which show that the spheres are of comparable volumes to the original NRs as shown in Figure 1b. The results of exposure to the nanosecond laser of the same energy (Figure 2b) show that only NRs absorbing at 800 nm seem to disappear with an increase in shorter NRs (absorbing at shorter wavelength between 550 and 700 nm). Increasing the energy of the nanosecond laser (see Figure 2c) leads to destruction of the whole NR distribution with a shift of the absorption at 800 nm to shorter NRs as well as to an increase in the spheres (absorption at 520 nm). The spheres are found to be of smaller size by TEM imaging, as shown in Figure 1c. Thus, fragmentation seems to occur in this energy range for exposure to long pulse-width lasers and 3 MW power. A femtosecond laser with much higher power (400 MW) does not fragment but seems to only melt the NRs within the inhomogeneous absorption distribution of the longitudinal band at 800 nm (see Figure 2a). If the power decreases by lowering the energy of the femtosecond pulses to 200 nJ (see Figure 2d), only NRs absorbing melt. This leads to narrowing of the inhomogeneous distribution of the NRs in solution, as shown from the narrowing of the absorption band width. This effect can be used to obtain a narrow distribution of nanorods by photothermal laser shaping. The higher power femtosecond laser pulses (Figure 2a) melt all the NRs absorbing within the inhomogeneously broadened distribution. This is a result of the high intensity of the high-power laser pulses which saturates the absorption of the NRs of different sizes having different cross sections within the uncertainty width of the 100 fs laser pulses.

From the above, one reaches the conclusion that with femtosecond lasers, the energy threshold of changing the gold NR shape is lower. This might suggest the importance of multiphoton absorption processes as the femtosecond excitation imports more energy per femtosecond pulse. However, comparing Figure 2a with 2b, even though we seem to excite all the inhomogeneous distribution with the femtosecond laser, the transformation is less drastic (melting) compared to the nanosecond process (fragmentation). Figure 2b shows that even at the low-energy (40 μJ) nanosecond excitation, fragmentation is taking place into smaller NRs. The decrease in the longitudinal absorption band intensity at the laser wavelength and the increase at long wavelength ($\sim$580 nm) support this type of transformation. These observations suggest that supplying the same (or even less) energy over longer periods of time leads to fragmentation.

There are two possible mechanisms that might explain the difference between the femtosecond and nanosecond laser irradiation effect of gold NRs. In the first mechanism, due to its higher power, the femtosecond laser introduces nonlinear processes leading to multiphoton ionization processes. Charge repulsion within the gold NR could lead to melting since transformation into a sphere minimizes the electrostatic repulsion between the charges in the ionized nanoparticles. Of course, a large increase in ionization at higher femtosecond energies should lead to explosion (i.e., fragmentation) after and even before melting. The nanosecond laser only heats the NRs and continues to heat the melted NRs until they fragment. It is well demonstrated[26,27] that in a number of gaseous molecules, femtosecond laser pulses lead to formation of the parent ions due to sequential multiphoton absorption (ladder mechanism)[26] while a nanosecond laser produces fragmented ions (ladder switching mechanism).[27] Indeed, an experiment with high-energy femtosecond excitation was carried out. The maximum energy of 1 mJ of our amplified Ti:Sapphire femtosecond system was used to irradiate the gold NRs. Again, transformation of the NRs into spherical particles of comparable volumes is observed. However, changing the position of the focusing lens and minimizing the spot size leads to fragmentation with the femtosecond laser pulses. The TEM images of the solution

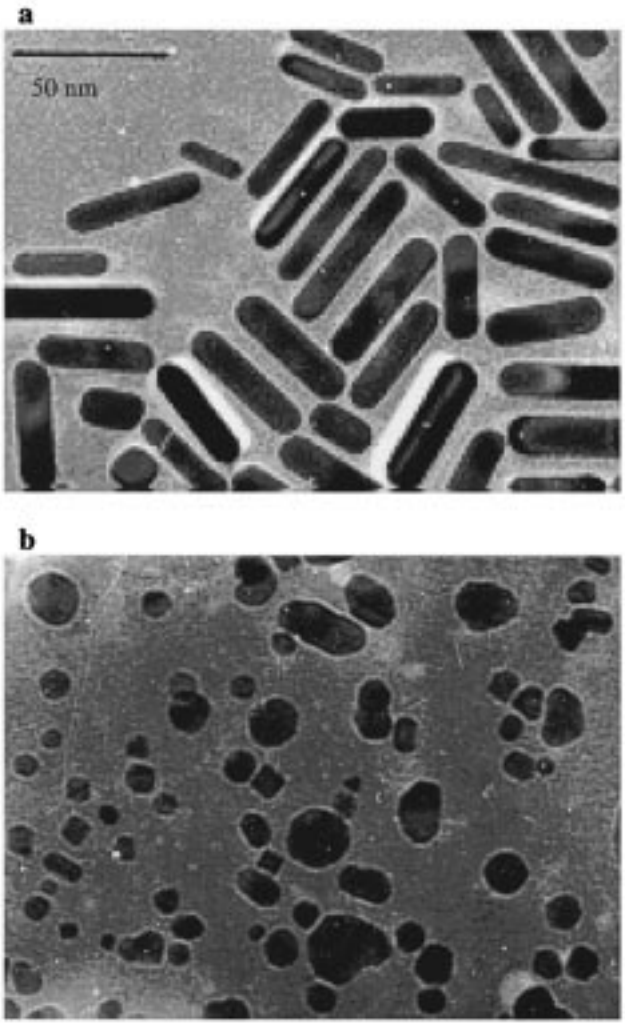

Figure 3. Effect of exposure of gold nanorods in micellar aqueous solution to high-energy high-power femtosecond laser pulses as determined by TEM images. (a) TEM image of the evaporated original solution prior to irradiation (mean aspect ratio of 4.1). (b) TEM image of the corresponding solution after exposure to tightly focused 1 mJ femtosecond pulses (800 nm, 100 fs). The particle shape is irregular, which suggests a rapid explosion of the gold nanorods after photoexcitation. (The scale bar in the upper left corner of (a) corresponds to 50 nm and also applies for (b).)

before and after the laser exposure are shown in Figure 3a and 3b, respectively. Fragmentation induced by high-energy (and also high power) femtosecond laser pulses is clearly observed. Some of the particles are found to have very irregular shapes, suggesting melting and dissociation taking place simultaneously. It should be noted that the power is so high that the cylindrical glass cell which contained the gold NR solution was also damaged in this experiment.

If the above mechanism is correct, one would have observed the characteristic solvated electron absorption at 700 nm on the picosecond time domain. We have not observed changes in this region of the spectrum when 1−40 ps time delays are used in our transient absorption experiments. Of course, the depletion of the absorption in the 800 nm region (due to the destruction of the NRs) could have interfered. However, temporal changes in the band shape (as the hydrated electron is solvated) should have been observed.

The second possible mechanism is that the initial absorption heats the electrons. This is known[28−31] to occur in gold nanoparticles on the femtosecond time domain. This is then followed by electron−phonon relaxation processes in the 1−3 ps time domain.[28−31] This leads to an increase in the gold atom kinetic energy and melting of the NRs. In the femtosecond irradiation, this occurs in the dark since the laser pulse width (100 fs) is shorter than the electron−phonon relaxation time (1−3 ps). In the nanosecond experiments, the hot molten spheres (or distorted NRs) are continuously bathed with light from the nanosecond laser pulse. These hot particles (spheres or distorted NRs) continue to absorb on the nanosecond time scale of the pulse and also lose some heat to the solvent (the measured phonon−phonon relaxation time is 100 ps). The latter process is a loss mechanism in the nanosecond experiment. However, the large increase in the irradiation time overcompensates for the amount of energy lost to the solvent in the high-energy nanosecond experiment (which fragments to small spheres) but not completely in the low-energy experiment (which gives short NRs). A summary of the proposed mechanism is given below:

$$(\mathrm{Au})_{\mathrm{NR}} \xrightarrow{n h\nu} [(\mathrm{Au})_{\mathrm{NR}}]^{\#} \quad (1)$$

$$[(\mathrm{Au})_{\mathrm{NR}}]^{\#} \xrightarrow{\mathrm{fs}} [(\mathrm{Au})_{\mathrm{NR}}]^{\perp} \quad (2)$$

$$[(\mathrm{Au})_{\mathrm{NR}}]^{\perp} \xrightarrow{\mathrm{ps}} [(\mathrm{Au})_{\mathrm{NR}}]^{\mathrm{vib}*} \quad (3)$$

$$[(\mathrm{Au})_{\mathrm{NR}}]^{\mathrm{vib}*} \xrightarrow{\mathrm{melting}} [(\mathrm{Au})_{\mathrm{NS}}] \quad (4)$$

$$[(\mathrm{Au})_{\mathrm{NP}}]^{\mathrm{vib}*} \xrightarrow{m h\nu(\mathrm{ns})} [(\mathrm{Au})_{\mathrm{NP}}]^{\mathrm{vib}**} \quad (5)$$

$$[(\mathrm{Au})_{\mathrm{NP}}]^{\mathrm{vib}**} \xrightarrow{\mathrm{fragmentation}} (\mathrm{Au})_{\mathrm{SNS}} \quad (6)$$

Processes 1, 2, and 3 represent laser excitation of the electrons, thermal heating of the electrons (occurring on the femtosecond time scale), and lattice (phonon) heating resulting from electron−phonon relaxation processes (occurring on the 1−3 ps time scale in gold nanocrystals[28−21]). NR, NS, NP, and SNS refer to nanorods, nanospheres, nanoparticles (when we are not sure if the particles are completely spherical or not), and small nanospheres, respectively. It is important to notice that heating the lattice via electron−phonon relaxation in the femtosecond experiment occurs in the dark, as it takes place in a time longer than the pulse width. This is not the case for the nanosecond experiments. Process 5 represents further laser excitation of the hot lattice in the experiments with nanosecond laser pulses. One thus expects that absorption of more photons by the hot lattice occurring in the nanosecond experiment is what leads to an increase in the lattice internal energy and fragmentation of the gold NRs (6).

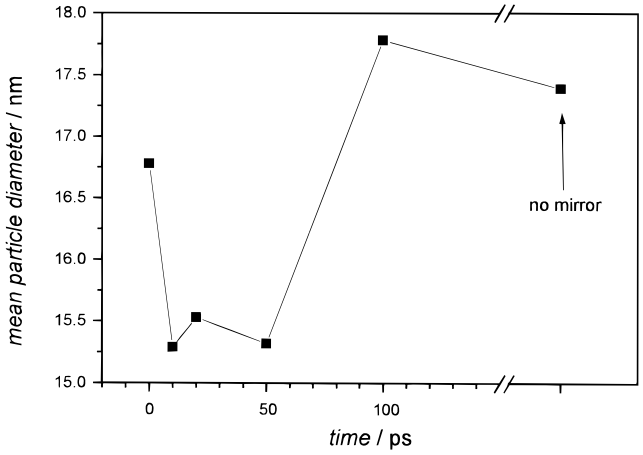

Figure 4. Dependence of the mean particle diameter on the time delay between two femtosecond laser pulses. The gold nanorod solution is exposed to 200 μJ femtosecond laser pulses, and the transmitted beam is passed through the sample again by reflecting it off a movable mirror behind the sample holder. The two beams are overlapped in the solution, and the mirror position was adjusted in μm steps corresponding to picosecond time resolution. It is found that the mean particle diameter of the spheres formed by laser irradiation is smallest for time delays between 10 and 50 ps due to a greater abundance of small spheres resulting from fragmentation of the nanorods. This corresponds well to the characteristic time scale during which the gold lattice is hot. These results support the suggested mechanism for photofragmentation of the gold nanorods with nanosecond laser pulses.

According to this mechanism, it is the hot spheres that need to be energized in order to fragment. Thus, irradiating the femtosecond-energized NRs with another femtosecond pulse after tens of picoseconds delay (to allow them to heat the nuclei) should lead to fragmentation. We performed a two-pulse experiment in which the gold NRs were irradiated with a femtosecond laser pulse which is refelcted back into the cell after different delay times using a movable mirror. The mirror was mounted on a μm translation stage behind the sample cell so that the two pulses, which are overlapped in the sample cell, could be time delayed with respect to each other. The pulse energy used was 200 μJ, and the optical density of the NR solution was adjusted to 0.2 in a cell with a 2 mm path length, thus attenuating the reflected beam by 37%. Neither the 200 μJ pulse nor a single pulse with the energy of the sum of the two pulses lead to photofragmentation, only melting of the NRs into spheres is observed in each experiment.

Figure 4 shows the results of this experiment. The mean diameter of the spheres formed is determined from the TEM images of each delay time and is plotted against the time delay between the two femtosecond pulses. For very short time delays (0 ps, mirror positioned as close as possible behind the sample cell) and for time delays longer than 100 ps, the mean particle diameter is comparable to the one found without the mirror. For intermediate time delays, a significantly smaller mean particle diameter is found due to a greater abundance of small spheres. This experiment was repeated twice. These results support the proposed mechanism as photofragmentation is found when the hot lattice absorbs additional photons by the second femtosecond pulse and that heating the lattice occurs in the picosecond time domain as determined from the time-resolved transient absorption measurement.[28−31] At times shorter than a few picoseconds (time for electron−phonon relaxation), the lattice is not hot, and at longer delay times than 100 ps (the

phonon−phonon relaxation time), absorbing another femtosecond pulse starts the process anew and only melting is observed. In this experiment, the nanosecond pulse is simulated by two femtosecond pulses.

According to the mechanism, increasing the energy of the femtosecond laser sufficiently, even in the dark, the heated molten spheres (or distorted NRs) can have sufficient energy to dissociate the particles. Thus, the results of Figure 3 can also be accounted for by this mechanism. Of course, multiphoton ionization processes must also be taking place to a certain extent and we cannot fully discard them.

Acknowledgment. This work was supported by the Office of Naval Research (Grant No. N00014-95-1-0306) and the ONR Molecular Design Institute at Georgia Tech. (Grant No. N00014-95-1-1116). S.L. thanks the German Fond der Chemischen Industrie and the German BMBF and M.B.M. the Egyptian GM for a Ph.D. fellowship, and C.B. thanks the DAAD for a postdoctoral fellowship.

References and Notes

(1) Alivisatos, A. P. *J. Phys. Chem.* **1996**, *100*, 13226.
(2) Henglein, A. *Chem. Rev.* **1989**, *89*, 1861.
(3) Melinon, P.; Paillard, V.; Dupuis, V.; Perez, A.; Jensen, P.; Hoareau, A.; Perez, J. P.; Tuaillon, J.; Broyer, M.; Vialle, J. L.; Pellarin, M.; Baguenard, B.; Lerme, J. *J. Mod. Phys. B* **1995**, *9*, 339.
(4) Alivisatos, A. P. *Science* **1996**, *271*, 933.
(5) Brus. L. E. *Appl. Phys. A* **1991**, *53*, 465.
(6) Schmidt, M.; Kusche, R.; Issendorff, B.; Haberland, H. *Nature* **1998**, *393*, 238.
(7) Lewis, L. J.; Jensen, P.; Barrat, J.-L. *Phys. Rev. B* **1997**, *56*, 2248.
(8) Ercolesi, F.; Andreoni, W.; Tosattie, E. *Phys. Rev. Lett.* **1991**, *66*, 911.
(9) Shi, F. G. *J. Mater. Res.* **1994**, *9*, 1307.
(10) Iijima, S.; Ichihashi, T. *Phys. Rev. Lett.* **1996**, *56*, 616.
(11) Smith, D. J.; Petford-Long, A. K.; Wallenberg, L. R.; Bovin, J.-O. *Science* **1996**, *233*, 872.
(12) Buffat, P.; Borel, J.-P. *Phys. Rev. A* **1976**, *13*, 2287.
(13) Ahmadi, T. S.; Wang, Z. L.; Green, T. C.; Henglein, A.; El-Sayed, M. A. *Science* **1996**, *272*, 1924.
(14) Wang, Z. L.; Petroski, J. M.; Green, T. C.; El-Sayed, M. A. *J. Phys. Chem. B* **1998**, *102*, 6145.
(15) Papavassiliou, G. C. *Prog. Solid State Chem*. **1980**, *12*, 185.
(16) Kerker, M. *The Scattering of Light and Other Electromagnetic Radiation*; Academic Press: New York, 1969.
(17) Bohren, C. F.; Huffman, D. R. *Absorption and Scattering of Light by Small Particles*; John Wiley: New York 1983.
(18) Kreibig, U.; Vollmer, M. *Optical Properties of Metal Clusters*; Springer: Berlin, 1995.
(19) Foss, C. A.; Hornyak, G. L.; Tierney, M. J.; Martin, C. R. *J. Phys. Chem.* **1992**, *96*, 9001.
(20) Martin, C. R. *Chem. Mater*. **1996**, *8*, 1739.
(21) v. d. Zande, B. M. I.; Bohmer, M. R.; Fokkink, L. G. J.; Schonenberger, C. *J. Phys. Chem. B* **1997**, *101*, 852.
(22) Yu, Y.; Chang, S.; Lee, C.; Wang, C. R. C. *J. Phys. Chem. B* **1997**, *101*, 6661.
(23) Kamat, P. V.; Flumiani, M.; Hartland, G. V. *J. Phys. Chem. B* **1998**, *102*, 3123.
(24) Kurita, H.; Takami, A.; Koda, S. *Appl. Phys. Lett.* **1998**, *72*, 789.
(25) Mohamed, M. B.; Link, S.; El-Sayed, M. A. *J. Phys. Chem. B* **1998**, *102*, 9370.
(26) . Yang, J. J.; Gobeli, D. A.; El-Sayed, M. A. *J. Phys. Chem.* **1985**, *89*, 3426.
(27) Gobeli, D. A.; Yang, J. J.; El-Sayed, M. A. *Chem. Rev*. **1985**, *85*, 529.
(28) Ahmadi, T. S.; Logunov, S. L.; El-Sayed, M. A. *J. Phys. Chem.* **1996**, *100*, 8053.
(29) Ahmadi, T. S.; Logunov, S. L.; El-Sayed, M. A.; Khoury, J. T.; Whetten, R. L. *J. Phys. Chem. B* **1997**, *101*, 3713.
(30) Perner, M.; Bost, P.; Plessen, G.; Feldmann, J.; Becker, U.; Mennig, M.; Schmidt, H. *Phys. Rev. Lett.* **1997**, *78*, 2192.
(31) Hodak, J. K.; Martini, I.; Hartland, G. V. *J. Phys. Chem. B* **1998**, *102*, 6958.